Published Online First: November, 2024
https://doi.org/10.21123/bsj.2024.10351
P-ISSN: 2078-8665 - E-ISSN: 2411-7986
Baghdad Science Journal

Probing the Morphology, Structure, and Optical Properties of Copper Samarium Borate Oxide Nanostructures

***Mohanad Q. Kareem* [*1], *Sarab M. Shareef* [2], *Maad M. Ameen* [1], *Sozan A. Hassan* [2], *Shaheen S. Alimardan*[1]**

[1] Department of Physics, College of Science, University of Kirkuk, Kirkuk, Iraq.
[2] Department of Physics, College of Pure Education, University of Kirkuk, Kirkuk, Iraq.
*Corresponding Author.

Received 02/12/2023, Revised 12/03/2024, Accepted 14/03/2024, Published Online First 20/11/2024

Abstract

The study prepared new Copper sodium borate oxide CSmBO nanocomposite thin films using a solvothermal synthesis method and the annealing process occurred at 350°C for 3 hours. The study characterized the films using FESEM, EDX, and UV spectroscopy. Based on the FESEM analysis, the films were uniform and dense, with nanoparticles which range from 21.49 to 96.51 nm in size. EDX confirmed the elemental composition of the CSmBO nanostructures, validating the successful incorporation of copper, samarium, and boron. (XRD) diffraction patterns show up that forming a Crystal phase with high levels of strain and blemish is due to nanoparticle gathering. The synthesized nanocomposites exhibited a remarkable tunability in morphology and structure. UV-Vis spectroscopy revealed a broad optical absorption spectrum with a maximum absorbance peak at 600 nm, demonstrating the potential of the CSmBO nanocomposite thin films for optoelectronic applications. The band gap (Eg) was 2.03 eV and the Urbach energy (Eu) 0.15 eV which indicates a relatively lower degree of localise band tail states. Successfully fabricating CSMBO nanocomposite thin films with tunable features highlights the potential of this composite for many optoelectronic implementation, inclusively solar energy harvesting, light-emitting and diodes photo catalysis.

Keywords: Copper Samarium Borate Oxide, Hydrothermal technique, Lanthanide, Morphology, Rare earth materials.

Introduction

The advancement of fundamental science, the development of innovative and the high-performance devices have been aided by the development of unique functional materials[1]. The creation of innovative functional materials and the construction of devices that use them are both difficult tasks that must begin with basic research[2,3] of the fundamental principles governing their synthesis, structure, and properties[4]. Two ways are feasible for achieving designated but unfulfilled functions. The first is to synthesize entirely new materials, while the second is to increase the quality of some previously existing materials by stacking them and then processing them in the nanoscale range. Because of its vast range of applications, wet-chemical synthesis has recently been used to create diverse sizes and shapes of distinct nonmaterial[3]. This endeavor often involves the exploration of various material classes, including

Published Online First: November, 2024
https://doi.org/10.21123/bsj.2024.10351
P-ISSN: 2078-8665 - E-ISSN: 2411-7986
Baghdad Science Journal

semiconductors, metals, ceramics, and polymers, each with its own unique set of properties and potential applications[5]. Rare earth compounds, characterized by their unique electronic configurations and rich chemical properties, have appeared as valuable materials for many applications[6]. These compounds, comprising elements from the lanthanide series, offer a diverse array of properties, including luminescence, magnetism, and catalytic activity[7,8], making them indispensable in various industries[9]. There are 17 rare earth elements[10]; all of which are found in the periodic table between lanthanum and lutetium. These elements are often grouped together because of their similar chemical properties[11]. Some of the most common rare earth compounds include Lanthanum oxide (La_2O_3), La_2O_3 is a white powder that is used in a diversity of implementations, involved glassmaking, ceramics, and catalysts[12]. Another element is the Cerium oxide (CeO_2) which is a yellow powder that is used in a diversity of implementations, involved polishing powders, catalysts, and fuel cells. Also, praseodymium oxide (Pr_6O_{11}) is a green powder that is used in a diversity of implementations, involved magnets, optical filters, and catalysts. Another element is neodymium oxide (Nd_2O_3) as a purple powder that is used in a various of implementations, inclusive magnets, lasers, and solar cells[13]. Then is the samarium oxide (Sm_2O_3) as brown powder that is used in a diversity of implementations[14], including magnets, lasers, and catalysts[15]. One of the many arrays of rare earth compounds[16] is Copper Samarium Borate Oxide CuSmBO as a favourable quaternary compound with wonderful features. This material, with the chemical formula CuSmBO4, shows a tetragonal crystal structure and have a 2.0 eV band gap. Its optics, In addition to being chemically stable and environmentally friendly, turn CuSmBO into an appealing material for different uses[17]. Synthesizing CuSmBO nanostructures has been extensively studied, using many techniques like solvothermal synthesis, hydrothermal installation[5], and solid-state installation[15,18.] Solvothermal synthesis, particularly, possesses protrude as a versatile and exceedingly utilized process for manufactured CuSmBO nanostructures which offers an exact Particle size control, morphology, and crystallinity. The synthesizing operator significantly affect the morphology, structures, and optical advantages of CuSmBO nanostructures. Particle sizes, shapes, and Crystal structures are organized by controlling temperatures, solvent, and reaction times. In addition, these factors influence the optical advantages, like absorbenc, emission, and energyband gap[19]. CuSmBO nanostructures have big potential for big optoelectronic uses due to their tunable optics. Their absorbance and emit light across a big spectral range suits for solar cells, light-emission diode (LED), photo-detectors, and sensors. Also, their photocatalytic features make them good nominees for environmental treatment and technologies of water purgation. This article characterizes, synthesizes, and possible CuSmBO nanostructure uses. It comprehensively overviewing tests rare earth combination which shows their unique properties and different uses. Then, CuSmBO by discussing its synthesis techniques, morphological features, structures, and optical advantages. Lastly, the possible application of CuSmBO nanostructures in many uses, such as the optoelectronics, environmental treatment and photo catalysis of providing a completely understanding CuSmBO nanoparticles Its ability to revolutionize many technological achievements. The focus is on the characterization, synthesis, and applications of these materials. This work contributes to the ongoing scholarly works on the nanomaterials and makes further discoveries possible. It describes the one-pot new copper samarium boride oxide nanocomposite film synthesis by the use of the hydrothermal method annealing at 350°C for 3 hours. It also discusses the structure, morphology, and optical features of this new Nanocomposite film.

Published Online First: November, 2024
https://doi.org/10.21123/bsj.2024.10351
P-ISSN: 2078-8665 - E-ISSN: 2411-7986
Baghdad Science Journal

Materials and Methods

Synthesis and Characterization of Copper Samarium Boride Oxide Nanocomposite.

Preparation of Samarium Boride Copper

Copper Samarium Boride Oxide (CuSmBO) nanocomposite was synthesized via a solvothermal method. The synthesis procedure involved the following steps: preparing the Reaction Mixture: 2.5 mmole of copper dichloride dehydrate ($CuCl_2 \cdot 2H_2O$, 99% purity, Sino Pharm Chemical Regent Co. Ltd., China) and 2.5 mmol of samarium trichloride hexahydrate ($SmCl_3 \cdot 6H_2O$, 99% purity, Changsha Eastham Co., Ltd., China) were melted in 50 mL of deionized water. A complexing agent and a reducing agent were added to the solution, followed by 0.25 g of sodium borohydride ($NaBH_4$, 98% purity, Sigma-Aldrich) and 0.1 g of poly (ethylene glycol) (PEG, 99% purity, Tianjin Guan Fu Chemical Research Institute Co., Ltd., China). The admixture was whiskered quickly at 45°C for 2 hours using a magnetic stirrer to ensure a complete dissolution of the precursors and formation of a uniform solution. Solvothermal Synthesis: The intended dissolution was a transmit to a Teflon-padded autoclave, filling it approximately to 60% of its volume. The autoclave was used to place the cleaned glass substrate, as the support for the CSmBO nanocomposite film, at an angle against the wall. Then, over 6 hours, the autoclave was closed tightly inserting it in a furnace at 175°C. This solvothermal treatment allowed the CSmBO nanocomposite to form and deposit onto the glass substrate. In the post-Synthesis Treatment, the solvothermal reaction was followed by the autoclave careful removal from the oven for cooling to (Rt) room temperature. The glass substrate was retrieved from the autoclave and thoroughly purified with deionized water and ethanol for the removal of any unreacted precursor residues. The washed substrate was then dried in a furnace at 70°C for 2 hours in order to ensure the evaporation of the solvents. The second step is the annealing process. These processes further enhance the crystallinity and optimize the optical properties of the CSmBO nanocomposite film and the annealed substrate was subjected to an annealing process. The substrate was placed in a preheated oven at 350°C, for 90 minutes. This annealing treatment rearranges CSmBO nanoparticles and form better organized crystalline structures, potential improvement of the film's performance in various optoelectronic achievements. The next process is description. Following the synthesis and post-synthesis treating, there are studies of the crystalline structures, Surface topography, and optical properties of the CSBO nanoparticles film Through various analytical mechanisms, X- ray diffraction, scanning electron microscopic (SEM), transmissions electron microscopic (TEM), and UV-vis Spectroscopic analysis. The characterization provided insights into the crystalline structures, Particle diameters, Surface topography, and optical absorption and emission CuSmBO nanoparticles film countenance. This synthesis shows simple and efficient methods of preparing a high-quality CuSmBO nanoparticles film with controlled morphology and tunable optical properties which turns them promising for many opto-electronic achievement, in solar cells, light-emission diodes, and photo-detectors.

Instrumentation

The elemental synthesized Copper Samarium Boride Oxide CuSmBO nanoparticles composition structural features of the were widely characterized by a suite of progressive analytics mechanisms. PAN analytics X'Pert High Score Plus Diffraction meter was used to examine the crystalline structure. It also tested phase purity of the CuSmBO nanocomposite with Cu-Kα eradiation (λ = 1.5406 Å). The deviation patterns were collected at room temperature with a stride size of 0.02° and a scan average of 0.1°/min. The obtained diffraction data was analyzed using the Rietveld refinement method to locate the lattice parameters, crystal symmetry, and phase composition of the CuSmBO nanocomposite. The surface morphology and micro-structure of the CuSmBO nanocomposite have been studied by a FE-SEM instrument (Quanta 200, FEI, America). The FE-SEM images were acquired at high magnification to reveal the Particle diameter, shape, and

Published Online First: November, 2024
https://doi.org/10.21123/bsj.2024.10351
P-ISSN: 2078-8665 - E-ISSN: 2411-7986
Baghdad Science Journal

apportionment of the CuSmBO Nano synthesis. Additionally, the electron dispersive X-ray Spectroscopic analysis (EDX) was the procedure using the FE-SEM to determine the elemental composition of the CuSmBO nanocomposite. The optical absorption features of the CuSmBO nanocomposite thin film were studied by a double-beam UV-Vis spectra-photometer (SHIMADZU UV2600, Tokyo, Japan). The UV-Vis absorption spectrum was registered in the extent of 200 to 800 nm to specify the band gap Bg energy and absorption characteristics of the CuSmBO nanocomposite. The absorption spectra Submitted insights into the potential optoelectronic implementations of the CuSmBO nanocomposite. The descriptions supplied a great insights about the structure, morphological, and optical properties of the CuSmBO nanocomposites which Availability a inclusive understanding of its potential For many applications.

Results and Discussion

Scanning electron microscope (SEM)

Figure 1 is the Copper Samarium Borate Oxide CuSmBO nanoparticles composition scanning electron microscopy (SEM) images thin film which hydrothermal synthesis creates and annealed at 350°C over 90 minutes. The high-resolution image in Figure 1 (A) synthesis is a homogeneous pattern which indicate a uniform of nanoparticles, conglomerated formed on the glass. The low-resolution image and enlargement in Figure 1 (B) and Figure 1 (C) reveal the film is uniform and dense. The particles in the CuSmBO thin film are in the nanostructure range, with sizes of 21.49 to 96.51 nm. The homogeneity of the SEM images shows successful hydrothermal synthesis which forms a uniform CuSmBO thin film on the glass substrates. The nanoparticle agglomeration is a shared in nanomaterials, which is primarily driven by the high nanoparticle surface energies. This conglomerated influences the film's features, like its electrical conductivity and mechanical strength. More studies could study strategies to control nanoparticle size and conglomerated to optimize the film's features. The low-resolution images in Figure 1 (B) and Figure 1 (C) show broader views of the film's morphology which confirms its similarity and dense packing. The large pore or gap lack indicates a well-structured and nonstop film. This uniform morphology is conclusive to achieve coveted features, like better mechanical strengths and electrical conductivity[20].

The nanostructure of the CuSmBO thin film is used for different purposes enhancing the surface areas and reactivity of the substances. The EDX in Figure **1** the CuSmBO thin film (D) analyses by hydrothermal techniques and annealed at 350°C over 180 minutes shows two peaks for copper (Cu) at 0.8 and 8.8 Kev which are the Lα and K_{α}, K_{β} transitions, respectively. Boron (B) peaks are at 2.1, 2.7, and 5.6 Kev, at L_{β}, L_{α} and $L_{\beta 2}$ transitions. Samarium (Sm) peaks are 2.6, 3.7, 6.2, and 7.1 Kev which are the K_{α}, L_{β}, $L_{\beta 2}$ and $L_{\gamma 1}$ transitions. Oxygen (O) peaks are observed at 0.5 Kev, being the K_{α} transition[21]. The EDS analyses proves that there is copper, samarium, boron, and oxygen in the CuSmBO thin film. The relative peak intensities entail that copper is the major the thin film element, followed by samarium, boron, and oxygen. The SEM images is the particle diameter of the CuSmBO thin film which increases with the annealing temperature because of the risen diffusion of atoms and the figuration of larger crystallites at high temperatures. Also, EDS analysis shows the relative peak intensity of copper rises with the annealing temperatures because of the discriminatory dispersion of copper atoms to the surface of the thin film at high temperatures. Differences in the SEM images and EDS analyses can happen due to some factors, such as the specified hydrothermal synthesis situations, the annealing temperature and time, the thickness of the thin film and the impurities[22].

Published Online First: November, 2024
https://doi.org/10.21123/bsj.2024.10351
P-ISSN: 2078-8665 - E-ISSN: 2411-7986
Baghdad Science Journal

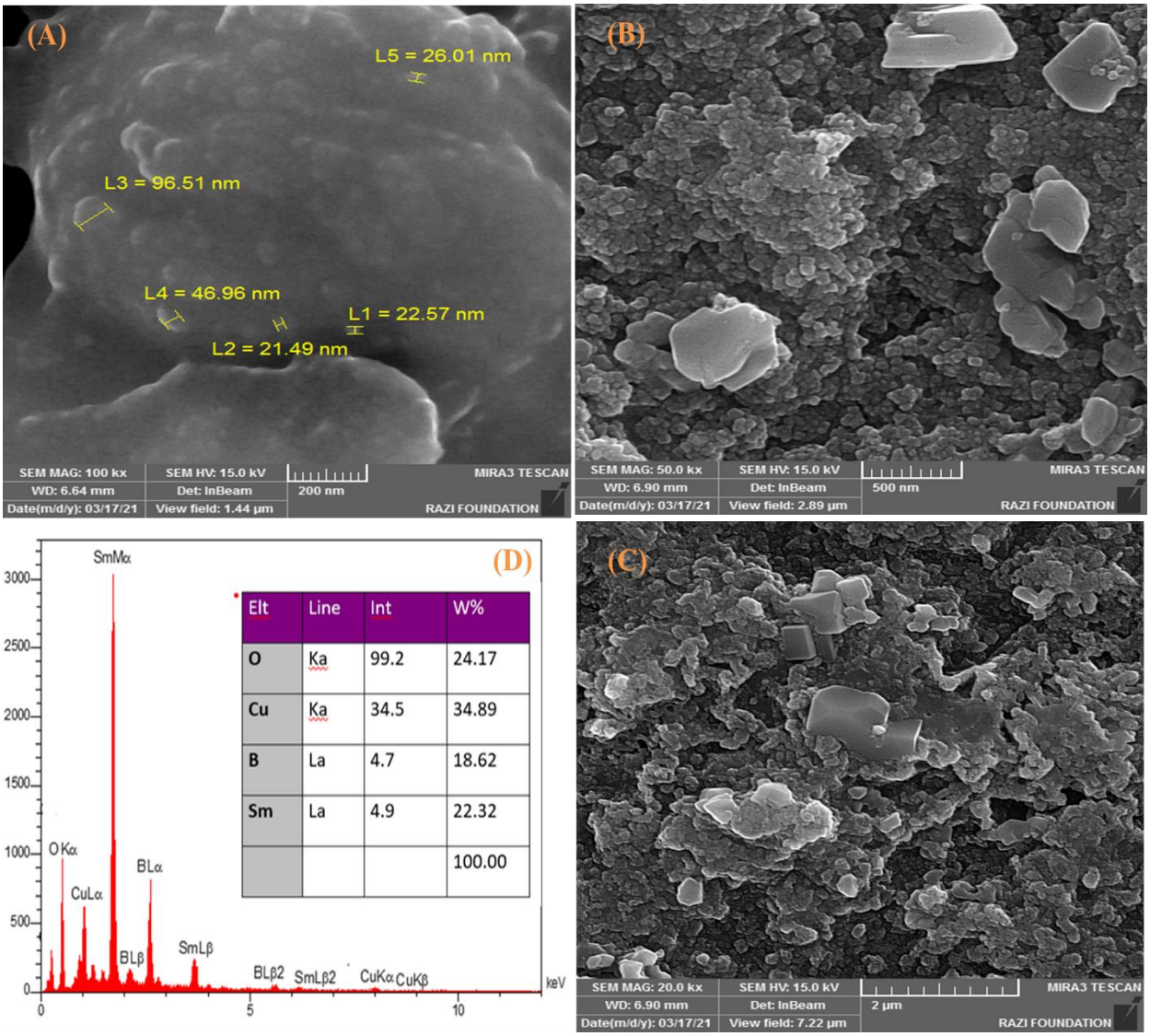

Figure 1. SEM of Copper Samarium Borate Oxide CuSmBO nanoparticles composition thin film prepared by hydrothermal mechanism, that annealing at 350ºC for 3 hr .(A, B and C) Surface morphology, ((A) high-resolution image), (B and C) inset: low-resolution image and magnification and (D) EDX analysis of CuSmBO nanoparticles composition thin film.

Overall, the SEM images and EDX analyses reveal the hydrothermal mechanism as simple and effective to prepare thin films of CuSmBO nanoparticles composition. The annealing temperature 350°C is sufficient for crystallizing the nanoparticles and forming a dense and uniform film. The nanoparticles in the film conglomerate, possibly due to the height Nanobodies surface energy [23].

Crystallography and X ray deviation (XRD) analysis.

We see from Figure 2 that the X ray pattern of the Copper Samarium Borate Oxide Nanocomposite thin film was annealed at 350°C. The XRD analysis of the Copper Samarium Borate Oxide Nanocomposite thin film revealed the presence of two distinct crystalline phases: Cu_5Sm and SmBO. The diffraction peaks observed in the XRD pattern match those reported in JCPDS cards for Cu_5Sm (JCPDS card No: 0933-065-03, coordinates 1524505) and SmBO (JCPDS card

Published Online First: November, 2024
https://doi.org/10.21123/bsj.2024.10351
P-ISSN: 2078-8665 - E-ISSN: 2411-7986
Baghdad Science Journal

No:7891-154-96, coordinates 1547890). These findings indicate that the hydrothermal synthesis process successfully produced a composite thin film containing both Cu_5Sm and SmBO phases. The Cu5Sm phase exhibits a hexagonal crystalline structure with a space set of P6/mm. The corresponding diffraction peaks were observed at angular positions (2θ) of 29.58°, 42.73°, and 61.4°, matching Miller indices (1 0 2), (3 0 0), and (2 1 2), respectively. The SmBO phase exhibits a monoclinic crystalline structure with a space group of C12/m 1.

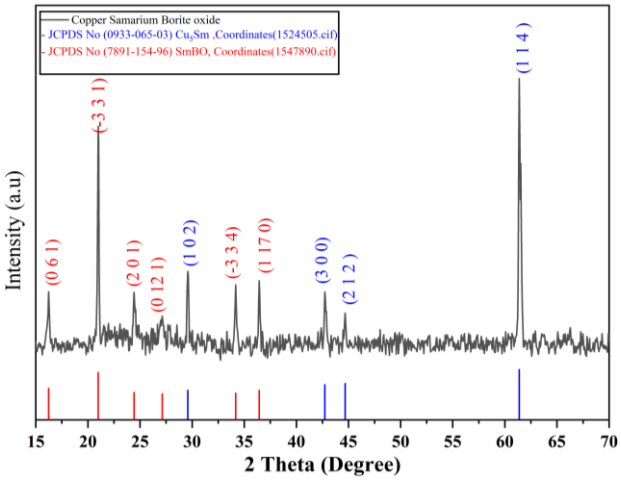

Figure 2.XRD diffraction pattern of Copper Samarium Borate Oxide Nano composite thin film by hydrothermal method, annealed at 350 ºC.

The corresponding diffraction peaks were observed at (2θ) positions of 16.23°, 20.98°, 24.43°, 27.13°, 34.18°, and 36.43°, matching Miller indices (0 6 1), (-3 3 1), (2 0 1), (0 12 1), (-3 3 4), and (1 17 0), respectively. The sharpness of the peaks in the X ray pattern indicates that the film is polycrystalline, composed of numerous tiny, crystalline grains. The absence of significant impurity peaks suggests that the film is predominantly composed of copper samarium borate oxide, with minimal impurities. An average crystal size of nanoparticles can be estimated using the Scherer Eq$\boldsymbol{Dsh = k\lambda/(\beta hkl\ cos\theta)}$ **1** [24,25]:

Table **1** which presents the structural and physical parameters of Copper Samarium Borate Oxide Nano composite thin film manufactured via the hydrothermal process and subsequently annealed at 350°C. The data includes a deviation angle (2θ), a full width at half maximum (FWHM), an estimated interplanar spacing (dhkl exp), a crystallite size (Dsh), a standard interplanar spacing (dhkl std.), Miller indices (hkl), a phase, crystal system, and JCPDS card number values suggesting higher

$$\boldsymbol{Dsh = k\lambda/(\beta hkl\ cos\theta)} \quad \textbf{1}$$

In the above equation, Dsh is the crystalline size, k a constant (usually 0.9), λ the wavelength of the Xrd. eradiation (0.15406 Å for Cu Kα eradiation), β the full width at half maximum (FWHM) of the deviation peak, and θ the deviation angle.

By measuring the FWHM of the deviation peaks and using the Scherer equation Eq$\boldsymbol{Dsh = k\lambda/(\beta hkl\ cos\theta)}$ **1**, the intermediate crystal size can be determined. This information can provide insights into the film's microstructure and properties. The calculated crystallite size for the Cu5Sm phase is 24.5 nm, and for the SmBO phase 18.7 nm. These values are somehow small, so the film has monocrystalline grains. The XRD pattern of the film reveals some trends: the (114) peak intensity at 61.4° significantly higher than the others. So, the (114) plane is the preferred. Also, the FWHM of the peaks varies, with the (114) peak having the smallest FWHM indicating the (114) grain largest and most well-ordered sizes in the film. This is due to the growth process. During hydrothermal synthesis, the film grows on a substrate. The substrate can influence the orientation of the film grains by providing a template for growth. The variation in the FWHM of the peaks is because of the difference in the size and grain crystallinity. Larger and more well-ordered grains typically have a smaller FWHM. The XRD analysis confirms the successful synthesis of a highly crystalline Copper Samarium Borate Oxide Nano composite thin film with the desired monoclinic crystal structure. The intermediate crystallite size of the nanoparticles in the film is estimated to be around 25 nm, in agreement with the SEM observations. This crystalline nature and well-defined crystal structure are essential for achieving the desirable features and performance of the nanocomposite thin film in various applications.

The results are offered in

Published Online First: November, 2024
https://doi.org/10.21123/bsj.2024.10351
P-ISSN: 2078-8665 - E-ISSN: 2411-7986
Baghdad Science Journal

crystallinity.

Table 1.The data on structural and physical variable of Copper Samarium Borate Oxide CuSmBO nanoparticles thin films.

2θ (Deg)	FWHM (Deg)	d_{hkl} Exp.(Å)	Dsh (nm)	d_{hkl} Std.(Å)	hkl	Phase	Crystal system	card number
16.2300	0.3200	3.4957	25.1	3.52755	0 6 1	SmBO	Monoclinic	7891-154-96
20.9800	0.5400	2.7226	15.0	2.73017	-3 3 1	SmBO	Monoclinic	7891-154-96
24.4300	0.6540	2.3380	12.4	2.3235	201	SmBO	Monoclinic	7891-154-96
27.1300	0.4320	2.1302	18.9	2.1076	0 12 1	SmBO	Monoclinic	7891-154-96
29.5800	0.4730	1.9282	17.4	1.9335	102	Cu5Sm	Hexagonal	0933-065-03
34.1800	0.5120	1.6701	16.2	1.6667	-3 3 4	SmBO	Monoclinic	7891-154-96
36.4300	0.6320	1.5651	13.2	1.5781	1 17 0	SmBO	Monoclinic	7891-154-96
42.7300	0.4830	1.3711	17.7	1.3461	300	Cu5Sm	Hexagonal	0933-065-03
44.6800	0.4310	1.3141	19.9	1.2841	212	Cu5Sm	Hexagonal	0933-065-03
61.38	0.364	0.97866	25.388	0.9337	114	Cu5Sm	Hexagonal	0933-065-03

The estimated interplanar spacing (d_{hkl} exp.) is calculated from the 2θ values using the Bragg's law and reflects the arranging of atoms within the crystalline lattice.

The diffraction angle (2θ) values correspond to the specific crystal planes within the nanocomposite thin film. The full width at half maximum (FWHM) indicates the degree of crystallinity, with narrower FWHM. The crystallite size (Dsh) is estimated using the Scherer Eq$\boldsymbol{Dsh = k\lambda/(\beta hkl\ cos\theta)}$ ***1*** , which relates the Table ***1*** suggest a correlation between the FWHM values and the crystallite sizes. Narrower FWHM values correspond to larger crystallite sizes, indicating a higher degree of crystallinity[27].This trend is the variances in the estimated interplanar spacing (d_{hkl} exp.) compared to the standard Table ***1*** confirms the successful synthesis of a nano crystalline Copper Samarium Borate Oxide Nano composite thin film with a mixed phase composition of SmBO and Cu_5Sm. The estimated crystallite sizes, ranging from 12.4 nm to 25.3 nm, indicate a nanoscale structure. The observed trends and variances in the diffraction data provide insights into the crystallinity and structural imperfections within the nanocomposite thin film. These structural characteristics can influence the material's properties and potential applications.

FWHM to the crystallite size [26] .The obtained crystallite sizes range from 12.4 nm to 25.3 nm, indicating a monocrystalline structure Phase Identification. The Miller indices (hkl) provide information about the specific crystal planes contributing to each diffraction peak. The phase is identified as either SmBO (samarium borate oxide) or Cu_5Sm (copper samarium) based on the JCPDS card numbers. The crystal system is determined as either monoclinic or hexagonal. The observed trends in

interplanar spacing (d_{hkl} std.) which could arise from the lattice strains or defects within the nanocomposite thin film. These imperfections can affect the diffraction patterns and lead to slight deviations from the expected interplanar spacing. The data in

Published Online First: November, 2024
https://doi.org/10.21123/bsj.2024.10351
P-ISSN: 2078-8665 - E-ISSN: 2411-7986
Baghdad Science Journal

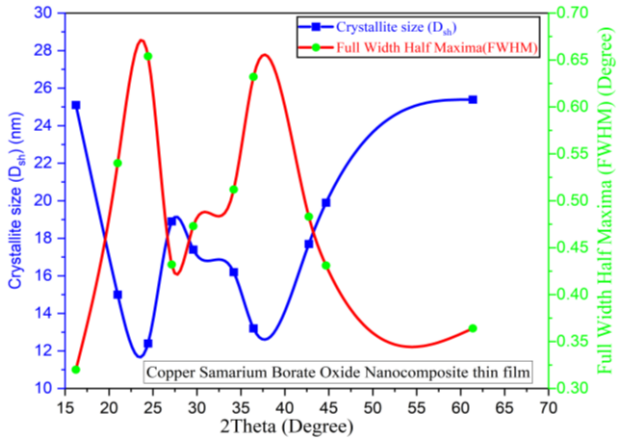

Figure 3. Variation of crystallite size (Dsh), Full Width Half Maxima (FWHM) versus (2Theta) of Copper Samarium Borate Oxide nanocomposite annealed 3 hours.

Figure 3 shows two distinct trends: Crystallite size drops with the rise of(2θ). This trend matches the Scherer equation, which states that the crystallite size is negatively proportionate to the FWHM of the deviation peak. The FWHM of the deviation peak typically increases with the growing (2θ), due to the growth in strain and defects in the crystal lattice [28] . As a result, the crystallite size decreases when (2θ) increases. FWHM increases with the rise of (2θ). This trend is also consistent with the Scherer equation, as mentioned above. Additionally, the rise in FWHM with the rise (2θ) is possibly attributed to the rising number of diffraction peaks at higher (2θ) angles.

The trends observed in Figure 3 have several implications for the properties of the Copper Samarium Borate Oxide nanocomposite thin film. The reduction in crystalline size with the increasing (2θ) proposes that the film is composed of monocrystalline grains. Nano crystalline materials usually show improvement of the mechanical features, like high strength and hardness. Additionally, nanocrystalline materials can have improved electrical conductivity and optical properties. The increase in FWHM with the increasing (2θ) suggests that the film possesses large degrees of strain and defects. This can negatively impact the mechanistic features of the film, such as reducing its strength and toughness.[29,30]. However, the high degrees of strain and defects can also improve electrical conductivity and optical properties.

Optical study results

The energy gap of a semiconductor material is a crucial parameter to determine how suitable it is for optoelectronic uses. For instance, semiconductors with wider energy gaps are more transparent to visible light and are therefore preferred for solar cell applications. On the other hand, semiconductors with narrower energy gaps are more efficient at absorbing visible light and are therefore preferred for light-emitting diode (LED) applications[31]. Figure 4 presents the absorbance spectrum of the Copper Samarium Borate Oxide Nano composite thin film annealed at 350 °C for 3 hours

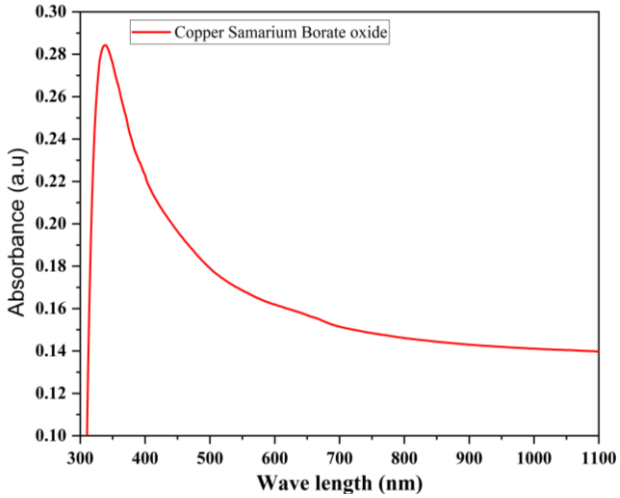

Figure 4.The absorbance as a function of the wavelength of the prepared Copper Samarium Borate Oxide Nano composite thin film that annealing at 350 °C for 3 hr.

The spectrum shows a wide absorption band in the visional and near-infrared (NIR) zones, with an eventual absorbance peak at approximately 600 nm. The wide absorption band is because of the electronic transitions of the Cu_{2+} and Sm_{3+} ions in the Copper Samarium Borate Oxide CuSmBO nanoparticles thin film[31]. The Cu_{2+} ions may encounter a transmission from the ground to the excited states resulting in the absorption of visible lights. The Sm_{3+} ions encounter an f-f transition from the ground to the excited states, which leads to the absorbing NIR lights. The maximum absorbance peak at 350 nm is due to the d-d transition of the Cu_{2+} ions. This transition is the

Published Online First: November, 2024
https://doi.org/10.21123/bsj.2024.10351
P-ISSN: 2078-8665 - E-ISSN: 2411-7986
Baghdad Science Journal

"spin-allowed" transition, characterized by a high absorption likelihood. The absorption band broadness is because of the different Cu_{2+} sites in the nanocomposite thin film, each with slightly various energy levels. The wide absorption band in the visible and NIR areas indicate that the Copper Samarium Borate Oxide nanoparticles thin film is a light absorber for a solar energy which harvests and photo catalyze uses. To absorb many wavelengths enables an efficient sunlight use, improving performance in these uses. Also, the high absorption in the NIR region is a positive use in optical sensing and high-resolution imaging. NIR light is less vulnerable to scatter and absorption by various biological tissues biological tissues This makes it ideal for deep tissue penetration, imaging and sensing. In general, the energy gap value 2.03 eV for the Copper Samarium Borate Oxide CuSmBO nanoparticles thin film annealed at 350 °C over 90 minutes shows potential for many optoelectronic uses.

Energy gap (Eg)

The optical energy gap was measured by Eq 2 and since the values of the absorption coefficient are greater than 4, the value of the constant (r) in Eq2 is 1/2 of the allowed direct transmission as shown in Eq *3*.

$$(\alpha h\upsilon) = B\left(h\upsilon - E_g\right)^r \qquad 2$$

$$(\alpha h\upsilon)^2 = \alpha_o\left(h\upsilon - E_g\right) \qquad 3$$

Figure 5 presents the energy gap value of the allowed direct transition of the Copper Samarium Borate Oxide CuSmBO nanoparticles thin film annealed at 350 °C for 3 hours.

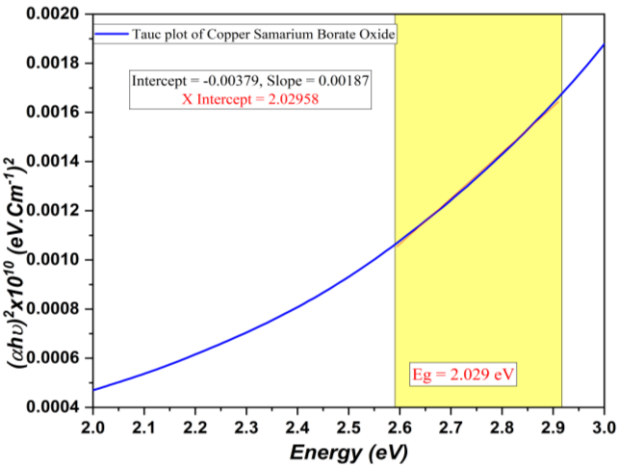

Figure 5. Plotting the energy gap value of the allowed direct transmission of the prepared Copper Samarium Borate Oxide Nano composite thin film that annealing at 350 °C for 3 hr.

This analysis provides a focused look into the fundamental optical features and potential implementation of the nanocomposite thin film. Estimating Energy Gap vi Tauc Plot, the energy gap (Eg) of the nanocomposite thin films was measured using the Tauc plot method. This method involves plotting the square of the absorption coefficient $(\alpha h\upsilon)^2$ against the photon energy ($h\nu$) and extrapolates the Linear part of the curve to the x-axis. The energy gap corresponds to the intercept of this linear extrapolation with the x-axis. The obtained energy gap amount of 2.03 eV indicates that the Copper Samarium Borate Oxide Nano composite thin film exhibits a semiconductor character with a moderate bandgap. This bandgap value is within the range of semiconductors suitable for a variety of optoelectronic applications. The Tauc plot analysis suggests that the observed absorption in the nanocomposite thin film corresponds to the allowed direct transition. This type of transition, characterized by a high absorption probability and a sharp absorption edge, is responsible for the observed linear relationship between $(\alpha h\upsilon)^2$ and $h\nu$ in the Tauc plot. The energy gap of a semiconductor is a critical parameter that determines its optical and electronic properties. Several factors contribute to the energy gap value, including (1) Chemical Composition where the energy levels of the valence and conduction bands, which dictate the energy gap,

Published Online First: November, 2024
https://doi.org/10.21123/bsj.2024.10351
P-ISSN: 2078-8665 - E-ISSN: 2411-7986
Baghdad Science Journal

are directly influenced by the chemical composition of the semiconductor material. (2) Crystal Structure: Here, the regulation of atoms during the crystalline lattice, characterized by the crystal structure, also affects the energy gap by influencing the band structure and electron interactions. (3) Impurities and Defects: The presence of impurities or defects can introduce additional energy levels within the bandgap, modifying the overall energy gap value. The energy gap of a semiconductor is crucial for determining whether it is suitable for many optoelectronic uses. Wider energy gaps generally lead to enhanced transparency and are preferred for solar cell applications, while narrower energy gaps favor light absorption and are suitable for light-emitting diodes (LEDs). The Copper Samarium Borate Oxide Nano composite thin film, with an energy gap of 2.03 eV, exhibits a balance between transparency and light absorption. This characteristic makes it a promising candidate for three opto-electronic implementations, including: (1) Solar Cells where the ability to absorb visible light while maintaining transparency is beneficial for harvesting solar energy and converting it into electricity in solar cells. (2) Light-Emitting Diodes (LEDs) is the moderate bandgap which allows for the efficient light emission at wavelengths within the visible range, making the nanocomposite a potential material for LEDs. (3) Photodetectors: in this application, the absorption of light can generate electron-hole pairs, enabling the nanocomposite to detect and respond to optical signals in photodetectors.

Urbach Energy (Eu)

The Urbach plot is characterized by a linear region at low photon energies, followed by a steep exponential cutoff at higher photon energies.

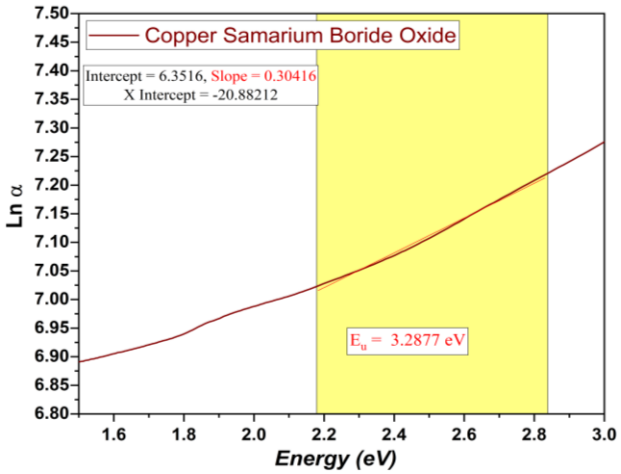

Figure 6. Plotting Lnα vs Energy of the prepared Copper Samarium Borate Oxide CuSmBO nanoparticles thin film that annealing at 350 ºC for 3 hr.

The linear region corresponds to the band tail states, which are energy levels within the band gap that arise because of the structural flaws and impurities. The slope of the linear region in the Urbach plot is called Auerbach energy (Eu), which represents the average energy separation between the band tail states and the band edge. The intercept of the linear region with the y-axis in the Urbach plot corresponds to the optical energy band gap (Eg) of the semiconductor materials. The optical energy band gap is the least energy wanted for exciting an electron to the conduction band from the valence band. Figure 6 presents a plot of the natural logarithm of the absorption coefficient (lnα) against the photon energy (hv) for the Copper Samarium Borate Oxide Nano composite thin film annealed at 350 °C for 3 hours. This plot, also known as the Urbach plot, is a useful tool for characterizing the band tailing and optical band gap of semiconductor substances. The Urbach energy of Copper Samarium Borate Oxide CuSmBO nanoparticles films annealed at 350ºC over 90 minutes was measured by Eq 4 ,Eq 5 [32].

$$\alpha = \alpha_o \exp\frac{h\upsilon}{E_u} \quad (4)$$

$$\ln \alpha = \ln \alpha_o + (\frac{h\upsilon}{E_u}) \quad (5)$$

Figure 6 shows the Urbach energy (Eu) diagram for thin CuSmBO nanoparticles with a linear region

Published Online First: November, 2024
https://doi.org/10.21123/bsj.2024.10351
P-ISSN: 2078-8665 - E-ISSN: 2411-7986
Baghdad Science Journal

at low energies and a large, sharp cutoff at higher energies. This corresponds to the well-defined band tail and optical band gap states in the nanoparticles thin film. The Urbach energy (Eu) value of the nanoscale thin films is approximately 0.15 eV. The relatively low Urbach energy value means that the band tail states are not important for localization, It is useful in transporting charge carriers in optoelectronics. The optical band gap value (Eg) for the nanoparticles films was 2.03 eV. This band gap value remained with the value by the Tauc plot in Figure 6. The suitable band gap of 2.03 eV makes the Copper Samarium Borate Oxide nanoparticles films adequate to many opto-electronic applications such as solar cells, LEDs, and photodetectors. This work provided insights into the important optoelectronic features of the Nano compound thin film and guide developing high-performance optoelectronic devices. In general, the Urbach plot in Figure 6 gives valuable insights into the band tailing and optical band gap of the Copper Samarium Borate Oxide Nano composite thin film. The moderate band gap 2.03 eV and the relatively low Urbach energy of 0.15 eV help the Nano compound thin film to be favorable to many optoelectronic implementations.

Conclusion

The solvothermal synthesis is a successful method creating a novel Copper Samarium Borate Oxide CuSmBO nanoparticles thin film subsequently annealed at 350°C for 180 minutes with adjustable morphologies, structures, and optical features. The characterization showed a grain size 22 nm, from 20.07 nm to 16.8 nm, which results in band gap energy 2.029 eV. The manufactured nanoparticles showed a wide optical absorption spectrum with a maximum absorbance peak at 600 nm which elucidates their advantages for optoelectronic uses. This method confirmed multilateral and efficient in manufacturing Copper Samarium Borate Oxide nanostructures with tunable features. A careful control synthesis features, nanoparticles with many morphologies are possibly nanoparticles, nanorods, and nanowires and are tailored. Also, the crystal structure is used, with forming monoclinic or hexagonal phases. The optimal morphology features, structure, and optics of Copper Samarium Borate Oxide CuSmBO nanoparticles rely in the specific optoelectronic implementation. For harvesting solar energy, nanoparticles with a big surface area and wide absorption bands are desirable. Photo catalysis needs nanoparticles with a high crystallinity and showed active positions. Light-emitting diodes need nanostructures with a tight band gap and an effective light emission. The solvothermal manufacturing method is promising path to produce Copper Samarium Borate Oxide nanostructure with Adjustable morphology features, structures, and optical properties. The meticulous control synthesis features help these nanostructures in tailoring for meeting some requirements of optoelectronic uses.

Authors' Declaration

- Conflicts of Interest: None.
- We hereby confirm that all the Figures and Tables in the manuscript are ours. Furthermore, any Figures and images, that are not ours, have been included with the necessary permission for re-publication, which is attached to the manuscript.
- No animal studies are present in the manuscript.
- No human studies are present in the manuscript.
- Ethical Clearance: The project was approved by the local ethical committee at University of Kirkuk.

Authors' Contribution Statement

The proposed idea was conceived by M. Q. K. The data was acquired by M. M. A and M. Q. K. The analysis was carried out by S. A. H., M. Q. K, and S. M. Sh. The data were interpreted by M. Q. K. The

Published Online First: November, 2024
https://doi.org/10.21123/bsj.2024.10351
P-ISSN: 2078-8665 - E-ISSN: 2411-7986
Baghdad Science Journal

paper's drafter is S.A.H. The article was revised and proofread by M. Q. K, M.M.A, and Sh. S.A. All authors read the manuscript carefully and approve the final version of their MS.

References

1. Tapak NS, Nawawi MA, Mohamed AH, Tjih ETT, Mohd Y, Rashid AHBA, et al. Chemical Synthesis of Metal Oxide Nanoparticles Via Ionic Liquid As Capping Agent: Principle, Preparation and Applications. Malaysian J Anal Sci MJAS 2022;26(6): 1394–1420. https://mjas.analis.com.my/mjas/v26_n6/pdf/Tapak_26_6_18.pdf .
2. Alam S, Chowdhury MA, Shahid A, Alam R, Rahim A. Synthesis of emerging two-dimensional (2D) materials – Advances, challenges and prospects. FlatChem. 2021; 30: 100305. https://doi.org/10.1016/j.flatc.2021.100305 .
3. Shaker DS, Abass NK, Ulwall RA. Preparation and study of the Structural, Morphological and Optical properties of pure Tin Oxide Nanoparticle doped with Cu. Baghdad Sci J. 2022; 0660-0660. http://dx.doi.org/10.21123/bsj.2022.19.3.0660 .45870eac05426706.pdf .
4. Khalaf WM, Al-Mashhadani MH. Synthesis and characterization of lanthanum oxide la2o3 net-like nanoparticles by new combustion method. Biointerface Res App. 2022; 12(3): 3066–3075. https://doi.org/10.33263/BRIAC123.30663075 .
5. Ubale SB, Ghogare TT, Lokhande VC, Ji T, Lokhande CD. Electrochemical behavior of hydrothermally synthesized porous groundnuts-like samarium oxide thin films. SN Appl Sci. 2020; 2(4):756. https://doi.org/10.1007/s42452-020-2467-z .
6. Filho WL, Kotter R, Özuyar PG, Abubakar IR, Eustachio JHPP, Matandirotya NR. Understanding Rare Earth Elements as Critical Raw Materials. Sustainability (Switzerland). 2023; 15(3): 1919. https://doi.org/10.3390/su15031919 .
7. Artiushenko O, da Silva RF, Zaitsev V. Recent advances in functional materials for rare earth recovery: A review. SM&T .Elsevier B.V. 2023; 37(August): e00681. https://doi.org/10.1016/j.susmat.2023.e00681 .
8. Purba FJ, Sitorus Z, Tarigan K, Siregar N. Enhanced photocatalytic activity of Cu2O/ZnO/GO nanocomposites on the methylene blue degradation. Baghdad Sci. J. 2024; 0062-0062. https://doi.org/10.21123/bsj.2023.8087 .
9. M. Q. Kareem, M. M. Ameen, S. A. Hassan, and S. M. Shareef.Synthesis of Tetrahedrite Zincian Nanocomposites via solvothermal process at low temperature. Ceram Int, vol. 50, no. 20, Part B, pp. 40005–40013, 2024, doi: https://doi.org/10.1016/j.ceramint.2024.07.385.
10. Balaram V, Rare earth elements: A review of applications, occurrence, exploration, analysis, recycling, and environmental impact. Geosci Front. Elsevier Ltd; 2019; 10(4): 1285–1303. https://doi.org/10.1016/j.gsf.2018.12.005.
11. Gurunath LN, Bidve A , Synthesis and Characterization of Lanthanum Oxide Doped Polyaniline (PANI/La 2 O 3). J Surv Fish Sci. 2023; 10(4S): 1023–1028. https://doi.org/10.17762/sfs.v10i4S.1124 .
12. Shah H, Afzal S, Usman M, Shahzad K, Ikhioya IL. Impact of Annealing Temperature on Lanthanum Erbium Telluride (La0.1Er0.2Te0.2) Nanoparticles Synthesized via Hydrothermal Approach. Adv J Chem A. 2023; 6(4): 342–351. https://doi.org/10.22034/AJCA.2023.407424.1386 .
13. Colera ES, Tardío M,Tabarés EG, Perea B, Crespillo ML, Muñoz-Santiuste JE, et al. Development of Luminescent Nd-Doped LaNbO Compound Thin Film Growth by Magnetron Sputtering for the Improvement of Solar Cells. Crystals. 2023; 13(2): 159 https://doi.org/10.3390/cryst13020159 .
14. Barad C, Kimmel G, Hayun H, Shamir D, Hirshberg K. Phase stability of nanocrystal line grains of rare-earth oxides (Sm2O3 and Eu2O3) confined in magnesia (MgO) matrix. mater 2020; 13(9): 2201. https://doi.org/10.3390/ma13092201
15. Balamurugan A, Sudha M, Surendhiran S, Anandarasu R, Ravikumar S, Syed Khadar YA. Hydrothermal synthesis of samarium (Sm) doped cerium oxide (CeO2) nanoparticles: Characterization and antibacterial activity. Mater Today: Proc. 2019: 3588–3594. https://doi.org/10.1016/j.matpr.2019.08.217 .
16. Mackie AJ, Dean JS, Goodall R. Material and magnetic properties of Sm2(Co, Fe, Cu, Zr)17 permanent magnets processed by Spark Plasma Sintering. J Alloys Compd. 2019; 770: 765–770. https://doi.org/10.1016/j.jallcom.2018.08.186 .
17. Khasim S, Ramakrishna BN, Pasha A, Manjunatha SO. Structural, Optical, Magnetic, and Electrical Properties of Samarium (Sm3+)-Doped Copper–Iron Oxide Ferrites for Possible Optoelectronic Applications. J Electron. Mater. 2024; 53(2): 801–814. https://doi.org/10.1007/s11664-023-10797-w .
18. Jamdar M, Goudarzi M, Dawi EA, Mahdi MA, Jasim LS, Salavati-Niasari M. Synthesis of SmMnO3/Sm2O3 nanocomposites as efficient photocatalysts for organic dye degradation by sol gel pechini method. Results Eng. 2024;21(December 2023): 101650. https://doi.org/10.1016/j.rineng.2023.101650 .
19. Li M, Wang N, Zhang S, Hu J, Xiao H, Gong H, et al. A review of the properties, synthesis and applications of lanthanum copper oxychalcogenides. J Phys D: Appl Phys. {IOP} Publishing; 2022; 55(27): 273002. https://doi.org/10.1088/1361-6463/ac4b71 .

Published Online First: November, 2024
https://doi.org/10.21123/bsj.2024.10351
P-ISSN: 2078-8665 - E-ISSN: 2411-7986
Baghdad Science Journal

20. Sadeq MS, Morshidy HY. Effect of samarium oxide on structural, optical and electrical properties of some alumino-borate glasses with constant copper chloride. J Rare Earths. 2020; 38(7): 770-775. https://doi.org/10.1016/j.jre.2019.11.003 .
21. Cosico JAM, Marquez MC. Sonochemically assisted samarium doped copper (I) oxide nanostructures as potential component in PN junction. Key Eng Mater. 2020; 853: 73-77. https://doi.org/10.4028/www.scientific.net/KEM.853.73 .
22. Borik M, Chislov A, Kulebyakin A, Lomonova E, Milovich F, Myzina V, et al. Phase Composition and Mechanical Properties of Sm2O3 Partially Stabilized Zirconia Crystals. [Online] Crystals. 2022; *12*(11): 1630 . https://doi.org/10.3390/cryst12111630 .
23. Narenthiran B, Manivannan S, Sharmila S, Shanmugavani A,Ramulu PJ. Influence of Samarium on Structural, Morphological, and Electrical Properties of Lithium Manganese Oxide. Adv Mater Sci Eng. 2023; 2023(special issue):10. https://doi.org/10.1155/2023/8331899 .
24. Kareem MQ. Study Optical Properties of (GA) Polysaccharide/Polyvinyl alcohol thin films. Tikrit j pure sci. 2018; 20(4): 120–124. https://www.iasj.net/iasj/download/6128c92a9e14107d .
25. Mahmoud ZH, Al-Bayati RA, Khadom AA. In situ Polymerization of Polyaniline/Samarium Oxide-Anatase Titanium Dioxide (PANI/Sm2O3-TiO2) Nanocomposite: Structure, Thermal and Dielectric Constant Supercapacitor Application Study. J Oleo Sci.2022; 71(2): 311–319. https://doi.org/10.5650/jos.ess21283 .
26. Lin J, Chen H, Kang J, Quan LN, Lin Z, Kong Q, et al. Copper(I)-Based Highly Emissive All-Inorganic Rare-Earth Halide Clusters. Matter . 2019; 1(1): 180–191. https://doi.org/10.1016/j.matt.2019.05.027 .
27. Jamdar M, Heydariyan Z, Alzaidy AH, Dawi EA, Salavati-Niasari M. Eco-friendly auto-combustion synthesis and characterization of SmMnO3/Sm2O3/Mn2O3 nanocomposites in the presence of saccharides and their application as photocatalyst for degradation of water-soluble organic pollutants. Arab J Chem. 2023; 16(12): 105342. https://doi.org/10.1016/j.arabjc.2023.105342 .
28. Srinet G, Sharma S, Kumar M, Anshul A. Structural and optical properties of Mg modified ZnO nanoparticles: An x-ray peak broadening analysis. Phys E: Low-Dimens Syst. Nanostruct 2021; 125(2021): 114381. https://doi.org/10.1016/j.physe.2020.114381 .
29. Zaid MHM, Sidek HAA, El-Mallawany R, Almasri KA, Matori KA. Synthesis and characterization of samarium doped calcium soda-lime-silicate glass derived wollastonite glass-ceramics. J. Mater. Res. Technol. [Internet]. J Mater Res Technol. 2020; 9(6): 13153–13160. https://doi.org/10.1016/j.jmrt.2020.09.058 .
30. Abdel- wahab M Sh , Ibrahim AM , Farghali AA, Tawfik WZ . Sputtered nanocrystalline samarium doped CuO photoelectrode for efficient photoelectrochemical water splitting. Mater Today Commun. 2023; 37: 107122.https://doi.org/10.1016/j.mtcomm.2023.107122 .
31. Kilic G, Issa Sh AM, Ilik E, Kilicoglu O, Issever UG, El-Mallawany R, et al. Physical, thermal, optical, structural and nuclear radiation shielding properties of Sm2O3 reinforced borotellurite glasses. [Online] Ceram. Int. 2021; 6154–6168. https://doi.org/10.1016/j.ceramint.2020.10.194 .
32. Kareem MQ, Hassan SA, Ameen MM. Doping Effect ((COCl2. 6H2O) & (CuCl2. 6H2O)) (2%) w/v on Optical Energy gap of (GA/PVA) composite films. Tikrit j pure sci. 2015; 20(1): 114–119. https://www.iasj.net/iasj/download/78c0eb6cf1a5dc61

Published Online First: November, 2024
https://doi.org/10.21123/bsj.2024.10351
P-ISSN: 2078-8665 - E-ISSN: 2411-7986
Baghdad Science Journal

استكشاف مورفولوجيا، البنية، والخصائص البصرية للمتراكب النانوي اوكسيد بورات سماريوم النحاس

مهند قادر كريم[1]، سراب محمد شريف[2]، معدمحمد امين[1] ، سوزان عبد الله حسن[2] ، شاهين صلاح الدين علي مردان[1]

[1] قسم الفيزياء، كلية العلوم، جامعة كركوك، كركوك، العراق.
[2] قسم الفيزياء، كلية التربية للعلوم الصرفة ، جامعة كركوك، كركوك، العراق.

الخلاصة

تضمنت الدراسة تحضير اغشية رقيقة من المتراكب النانوي الجديد اوكسيد بورون سماريوم النحاس (CSmBO) بنجاح باستخدام طريقة solvothermal الملدن عند 350 درجة مئوية لمدة 3 ساعات. وتم توصيفها باستخدام المجهر الإلكتروني الماسح للمجال (FESEM)، مطياف الأشعة السينية ذات طاقة التشتيت (EDX) ، ومطياف UV-VIS . كشف تحليل المجهر الإلكتروني الماسح للحقل (FESEM) عن اغشية موحدة وكثيفة مع جزيئات نانوية تتراوح في حجمها من 21.49 إلى 96.51 نانومتر. أكد مطياف الأشعة السينية ذات طاقة التشتيت (EDX) على التركيب العنصري للمتراكب النانوي (CSmBO) ، مما يثبت النجاح في دمج النحاس والسماريوم والبورون.أشارت أنماط حيود الأشعة السينية إلى تكوين مرحلة بلورية بدرجة عالية من الإجهاد والعيوب، وهو ما يعزى إلى تكتل الجسيمات النانوية. أظهرت المتراكبات النانوية المصنعة قابلية ضبط ملحوظة في الشكل والبنية. كما كشف مطياف UV-Visعن طيف امتصاص ضوئي واسعًا مع ذروة امتصاص قصوى عند 600 نانومتر، مما يدل على إمكانية استخدام الأفلام الرقيقة المركبة لأكسيد بورون سماريوم النحاس في تطبيقات الإلكترونيات الضوئية. قدرت الفجوة النطاقية الضوئية (Eg) بحوالي 2.03 الكترون فولت، وكانت طاقة Urbach (Eu) 0.15 الكترون فولت، مما يشير إلى درجة منخفضة نسبيًا من حالات ذيل النطاق الموضعي. يبرز التصنيع الناجح للأفلام الرقيقة المركبة لأكسيد بورون سماريوم النحاس بخصائص قابلة للضبط إمكانية استخدام هذا المركب لمجموعة متنوعة من التطبيقات الإلكترونيات الضوئية، بما في ذلك حصاد الطاقة الشمسية والتحفيز الضوئي والصمامات الثنائية الباعثة للضوء.

الكلمات المفتاحية: أوكسيد بورات سماريوم النحاس ,تقنية الهيدروثرمال, لانثانيد , مورفولوجيا , مواد الأتربة النادرة.